

# TRANSIENT BEAM-BEAM EFFECT DURING ELECTRON BUNCH REPLACEMENT IN THE EIC\*

J. Qiang<sup>†</sup>, LBNL, Berkeley, CA, USA

M. Blaskiewicz, Y. Luo, C. Montag, D. Xu, F. Willeke, BNL, Long Island, NY, USA

Y. Hao, MSU, East Lansing, Michigan, USA

## Abstract

The high luminosity, high polarization electron-ion collider (EIC) will provide great opportunities in nuclear physics study. In order to maintain high polarization, the electron beam will be replaced every few minutes during the collider operation. This frequent replacement of electron beams can affect proton beam quality during the collision. In this paper, we report on the study of the transient effect of electron beam replacement on proton beam emittance growth through strong-strong beam-beam simulation. The effects of electron beam injection imperfection will be included in the study.

## INTRODUCTION

The electron-ion collider (EIC) as a gluon microscope has been approved by the Department of Energy as the next major scientific facility that probes the detailed physics inside the nucleus with deep inelastic scattering using polarized high energy electron [1]. The EIC consists of two colliding rings, a hadron ring of 41-275 GeV and an electron storage ring of 5-18 GeV. To maintain high polarization of the electron bunch in the electron storage ring, one will replace each electron bunch in about every five minutes. When an electron bunch is kicked out, another electron bunch will be injected into the same electron bucket on orbit and on energy from the Rapid Cycling Synchrotron (RCS). Transient beam-beam effect during electron bunch replacement needs to be studied, especially possible proton emittance growth during this process.

The proton beam emittance growth due to the optics mismatch caused by a newly injected electron bunch can be expressed as a function of the beta-function of the bare lattice,  $\beta_0$ , and the beta-function as modified by the beam-beam interaction with the electron bunch,  $\beta_1$ , as:

$$\epsilon_1 = \frac{\epsilon_0}{2} \left( \frac{\beta_1}{\beta_0} + \frac{\beta_0}{\beta_1} \right),$$

where  $\epsilon_0$  is the unperturbed emittance, and  $\epsilon_1$  the resulting emittance after the replacement [1]. The analytically calculated relative emittance growth is less than  $10^{-3}$  for each bunch replacement. This estimate will be checked using self-consistent strong-strong beam simulations in this study. The effects of imperfect electron bunch injection and

the tolerance levels of imperfections will also be studied using the simulations.

## COMPUTATION MODEL

The transient effect from the electron beam replacement injection was simulated using a self-consistent strong-strong beam-beam code, BeamBeam3D [2, 3]. The BeamBeam3D is a parallel three-dimensional particle-in-cell code to model beam-beam effects in high-energy ring colliders. This code includes a self-consistent calculation of the electromagnetic forces (beam-beam forces) from two colliding beams (i.e. strong-strong modeling), a linear and nonlinear high-order transfer map model for beam transport between collision points, a stochastic map to treat radiation damping, quantum excitation, a single map to account for chromaticity effects, a feedback model, an impedance model, and a Bremsstrahlung model. Here, the beam-beam forces can be from head-on collision, offset collision, and crossing angle collision. These forces are calculated by solving the Poisson equation using a shifted integrated Green function method, which can be computed very efficiently using an FFT-based algorithm on a uniform grid. For the crossing angle collision, the particles are transformed from the laboratory frame into a boosted Lorentz frame following the procedure described by Hirata [4] and by Leunissen *et al.* [5], where the beam-beam forces are calculated the in the same way as the head-on collision. After the collision the particles are transformed back into the laboratory frame. The BeamBeam3D code can handle multiple bunches from each beam collision at multiple interaction points (IPs). The parallel implementation is done using a particle-field decomposition method to achieve a good load balance.

Crab cavities are used to compensate the geometric luminosity loss during the crossing angle collision [6-9]. To model the beam transport through the crab cavity, we assumed a thin lens approximation where the transfer map in the x-z plane is given by

$$x^{n+1} = x^n$$

$$Px^{n+1} = Px^n + \frac{qV}{E_s} \sin(\omega z^n / c)$$

$$z^{n+1} = z^n$$

$$\delta E^{n+1} = \delta E^n + \frac{qV}{E_s} \cos(\omega z^n / c) x^n,$$

where  $qV/E_s$  is the normalized voltage of the crab cavity and  $\omega$  is the angular frequency of the crab cavity. For a perfect compensation, the voltage of the crab cavity is:

\*Work supported by the Director of the Office of Science of the US Department of Energy under Contract no. DEAC02-05CH11231.  
<sup>†</sup>jqiang@lbl.gov

$$V = \frac{E_c \tan(\theta_c/2)}{q\omega\sqrt{\beta^*\beta_{cc}}}$$

## SIMULATION RESULTS

The design parameters used in the simulations are given in the Fig. 1. These design parameters were chosen to produce  $\sim 10^{34}/\text{cm}^2/\text{s}$  peak luminosity for the collision of a 10 GeV electron bunch and a 275 GeV proton bunch with 25 mrad crossing angle [10]. Pairs of crab cavities are used on both sides of the collision point to correct the crossing angle for both colliding beams. The transverse tune working points are optimized to avoid major resonances and beam emittance growth. The nominal beam-beam parameters for the electron beam are (0.088, 0.1), and (0.01, 0.012) for the proton beam. The large beam-beam parameters result in strong coherent beam-beam effects during the initial ten thousand turns after the electron bunch injection. Such effects can cause proton beam emittance growth due to the collective dynamic interactions between the electron beam and the proton beam.

	electron	proton
energy (GeV)	10	275
tune	(0.08, 0.06)	(0.228, 0.21)
# of particles ( $10^{11}$ )	1.72	0.69
unnorm. $\varepsilon$ (nm)	(20, 1.1)	(11.3, 1.0)
$\beta^*$ (cm)	(55, 5.6)	(80, 7.2)
beam-beam para.	(0.088, 0.1)	(0.01, 0.012)
chromaticity	(1, 1)	(1, 1)
damp. time (turn)	(4000, 4000, 2000)	
crab cavity freq. (MHz)	394	197

Figure 1: EIC design parameters used in simulations.

In the EIC design, every couple of minutes, a new highly polarized electron bunch will be injected into the collider to replace the old electron bunch. In the simulation, instead of simulating the old electron beam up to a few minutes, we only simulated the old electron beam up to 20,000 turns since the beam attained an equilibrium in the electron storage ring after these turns due to the radiation damping. A new electron bunch was injected on the axis after 20,000 turns. The upper two plots of Fig. 2 show the electron bunch's emittance evolution. The lower two plots of Fig. 2 show the proton bunch's emittance evolution with one electron bunch replacement. It is seen that both the old and the new electron bunches have similar emittance evolution with beam-beam interactions. The new injected electron beam attains the equilibrium emittance after ten thousand turns. For the proton bunch, although there is an increase of emittance, the trend of the proton beam evolution after the injection stays about the same. The proton beam emittances increased by less than 0.1% in the horizontal plane and about 0.2% in the vertical plane after the electron beam injection. The proton emittance growth rates keep the same before and after a new electron bunch is injected.

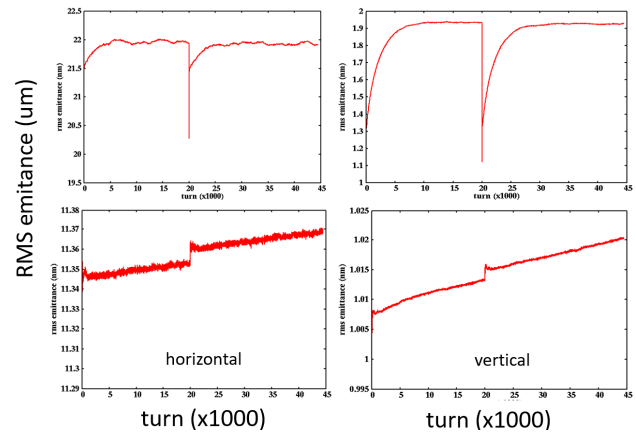


Figure 2: Simulated electron bunch horizontal (top left) and vertical (top right) emittance evolution and proton bunch horizontal (bottom left) and vertical (bottom right) emittance evolution during an electron bunch replacement injection at 20,000 turns. Injection error is not included.

In the above simulation, we assumed an ideal injection scenario. In the real accelerator operation, there will be imperfections during the injection. Those imperfections include initial centroid positions, angles, energy and time deviations, and electron beam size fluctuations. These imperfections, might result in extra proton beam emittance growth during electron bunch replacements.

Figure 3 shows proton beam horizontal and vertical emittance growth as a function of horizontal position and angle errors during the electron injection replacement. It is seen that in order to keep the proton beam emittance growth below 1% for a single electron bunch replacement, the electron beam injection horizontal centroid position error needs to be kept less than 0.6 sigma, or 60  $\mu\text{m}$  and the angle offset be less than 0.12 mrad.

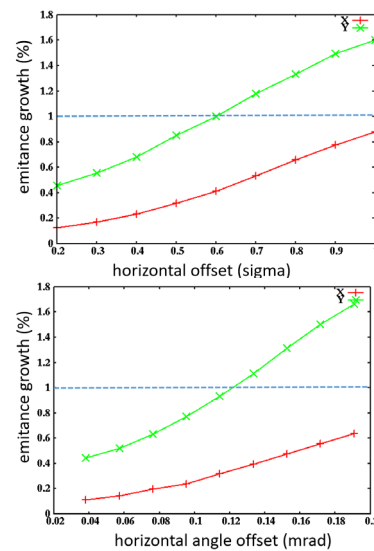


Figure 3: proton beam horizontal and vertical emittance growth as a function of horizontal position (top) and angle (bottom) errors of the electron injection replacement.

Figure 4 shows the proton beam emittance growth due to electron beam replacement as a function of the electron

Content from this work may be used under the terms of the CC BY 3.0 licence (© 2021). Any distribution of this work must maintain attribution to the author(s), title of the work, publisher, and DOI

beam vertical amplitude and angle errors. It is seen that the resulting proton beam emittance growth is small (less than 1%) even with up to one sigma vertical injection error. The proton beam horizontal emittance growth is not sensitive to these offset errors. The vertical emittance growth shows weak dependence on the offset error below 0.8 sigma. Here, one sigma corresponds to about 8  $\mu\text{m}$  of vertical rms beam size.

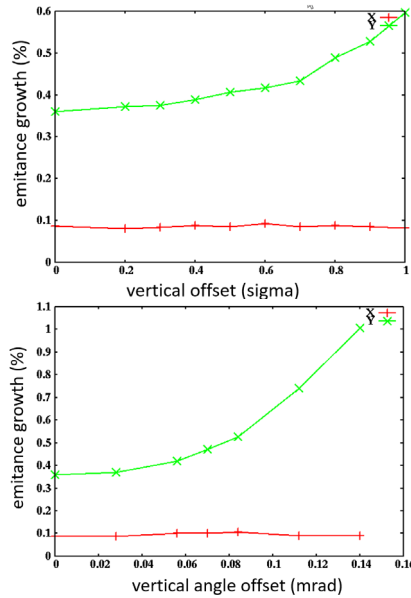


Figure 4: The proton beam emittance growth after electron beam replacement as a function of the electron beam vertical offset amplitude (top) and angle (bottom).

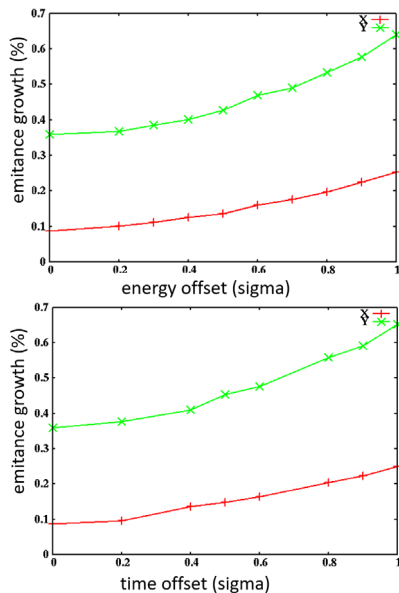


Figure 5: Proton beam horizontal and vertical emittance growth as a function of longitudinal energy (top) and time (bottom) offsets of the electron injection replacement.

Figure 5 shows proton beam horizontal and vertical emittance growth as a function of longitudinal energy and time errors of the electron injection. The impact of these

offsets on proton beam emittance growth is small (less than 1%) with a weak quadratic dependence.

Figure 6 shows proton beam horizontal and vertical emittance growth as a function of electron beam horizontal and vertical emittance mismatch factors of the electron injection replacement. The horizontal emittance growth is not very sensitive to the electron beam vertical emittance mismatch during the electron beam replacement injection. The proton beam emittance growth is small as long as the electron beam mismatch factor is above 0.6. In order to avoid the large proton beam emittance growth (>1%), the electron beam emittance mismatch factor should be sufficiently large (>0.8). The smaller mismatched electron beam produces stronger nonlinear beam-beam force and results in larger proton beam emittance growth.

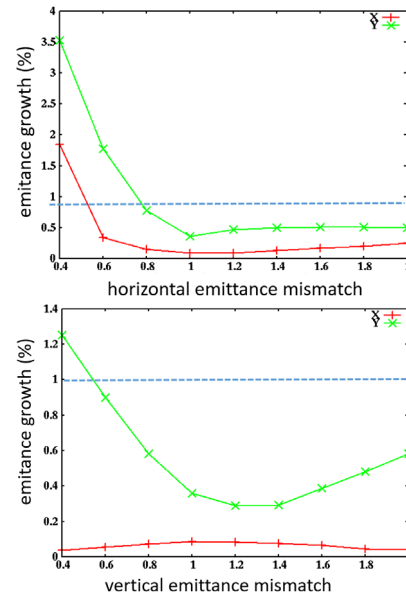


Figure 6: Proton beam horizontal and vertical emittance growth as a function of horizontal (top) and vertical (bottom) emittance mismatch factors of the electron injection replacement.

## SUMMARY

In this study, using the self-consistent strong-strong beam-beam simulations, we observed that electron beam replacement does not affect the proton beam emittance growth rate after the injection, but causes small emittance growth right after the injection due to the transient coherent beam-beam effects. The larger electron beam injection errors in general result in larger proton beam emittance growth. Horizontal offsets (centroid and angle) have larger impact on the proton beam emittance growth than the vertical offsets. Smaller emittance mismatch also has larger impact on the proton beam emittance growth than the larger mismatch factor. The effects of electron beam replacement on proton beam emittance can be small (<1%) with appropriate control of electron beam injection errors.

## REFERENCES

- [1] J. Beebe-Wang *et al.*, “Electron-Ion Collider Conceptual Design Report”, Brookhaven National Laboratory, Upton, NY, USA, Feb. 2021.
- [2] J. Qiang, M. A. Furman, and R. D. Ryne, “A parallel particle-in-cell model for beam-beam interaction in high energy ring colliders”, *Journal of Computational Physics*, vol. 198, no. 1, pp. 278–294, Jul. 2004. doi:10.1016/j.jcp.2004.01.008
- [3] J. Qiang, M. A. Furman, and R. D. Ryne, “Strong-strong beam-beam simulation using a Green function approach,” *Physical Review Special Topics - Accelerators and Beams*, vol. 5, no. 10, p. 104402, Oct. 2002. doi:10.1103/physrevstab.5.104402
- [4] K. Hirata, “Analysis of Beam-Beam Interactions with a Large Crossing Angle”, *Physical Review Letters*, vol. 74, no. 12, pp. 2228–2231, Mar. 1995. doi:10.1103/physrevlett.74.2228
- [5] L. H. A. Leunissen, F. Schmidt, and G. Ripken, “Six-dimensional beam-beam kick including coupled motion,” *Physical Review Special Topics - Accelerators and Beams*, vol. 3, no. 12, p. 124002, Dec. 2000. doi:10.1103/physrevstab.3.124002
- [6] R. B. Palmer, “Energy Scaling, Crab Crossing, and the Pair Problem”, presented at DPF Summer Study on High-energy Physics in the 1990s, Snowmass, CO, USA, Rep. SLAC-PUB-4707, Jul. 1988.
- [7] K. Oide and K. Yokoya, “Beam-beam collision scheme for storage-ring colliders”, *Physical Review A*, vol. 40, no. 1, pp. 315–316, Jul. 1989. doi:10.1103/physreva.40.315
- [8] K. Oide *et al.*, “Compensation of the Crossing Angle with Crab Cavities at KEKB”, in *Proc. 22nd Particle Accelerator Conf. (PAC’07)*, Albuquerque, NM, USA, Jun. 2007, paper MOZAKI01, pp. 27-31.
- [9] R. Calaga *et al.*, “Small Angle Crab Compensation for LHC IR Upgrade”, in *Proc. 22nd Particle Accelerator Conf. (PAC’07)*, Albuquerque, NM, USA, Jun. 2007, paper TUPAS089, pp. 1853-1855.
- [10] Y. Luo *et al.*, “Beam-Beam Related Design Parameter Optimization for the Electron-Ion Collider”, presented at the 12th Int. Particle Accelerator Conf. (IPAC’21), Campinas, Brazil, May 2021, paper THPAB028, this conference.